

FREQUENCY AND BANDWIDTH AGILE PULSER FOR USE IN ELECTRICAL AND BIOLOGICAL EFFECTS TESTING *

Michael C. Skipper, Michael D. Abdalla, and Samuel P. Romero

ASR Corporation, 7817 Bursara NW
Albuquerque, NM 87120

J. Scott Tyo

ECE Department, University of New Mexico
Albuquerque, NM 87131

Abstract

In this paper we present a Blumlein based pulse generator designed to be tunable in both center frequency and bandwidth. The pulser is designed around a parallel plate Blumlein configuration with a moveable center conductor. The pulse width is determined by moving the center conductor in and out of the Blumlein region, and the bandwidth is set by offsetting the center conductor towards one or the other of the outer electrodes. The output is designed to drive a test volume with cross sectional area on the order of 1 cm^2 . The final system will be capable of producing fields on the order of 30 kV/cm and will be useful for testing the interaction of high field, pulsed electromagnetic energy with small-scale electrical and biological systems. A low voltage experimental arrangement will be presented in this paper.

I. INTRODUCTION

One of the drawbacks of most sources used for effects testing is their lack of agility. In order to test a large region of the parameter space, we would like to be able to control the waveform, i.e. the center frequency and bandwidth of the output pulse. The pulser we have designed can produce a damped sine ringing waveform or a pulse that looks like a double exponential depending upon changeable Blumlein characteristics only. As a result, the exterior lines, including load line, will stay constant for ease of use.

II. EXPERIMENTAL ARRANGEMENT

The general source topology selected for this source is a Blumlein connected to a load parallel plate transmission line as shown in Figure 1. It is anticipated that the load line will be reduced (with constant impedance) in cross section to approximately 1 cm in height in the test volume region. The Blumlein will be pulse charged using high density DC-DC converter and a stacked solid-state switch. Each of the major component systems is discussed below.

A. Pulse Charging System

The ultimate Blumlein will be charged to 30 kV using an in-house designed high-voltage modulator. The prime power source will be a Tenma adjustable 30-V-DC power supply that will provide 24 VDC to the input of an Ultravolt model 30A24-P30-M DC-DC converter. The Ultravolt converter will charge a 1.7 nF TDK UHV-12A capacitor. The capacitor will then be switched to the Blumlein using a Behlke model HTS-300 stacked FET switch. The entire pulse charging system will be capable of operating a PRR of greater than 10 kHz . For our preliminary experiments reported here, the center conductor was DC charged to 130 V using an Ultravolt 1C24-P125 DC-DC converter, and the switch used was a 2N2222 triggered transistor. Output voltage measurements were made with a capacitive voltage probe situated on the bottom electrode.

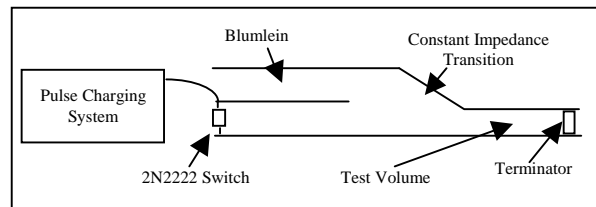


Figure 1: General experimental source topology.

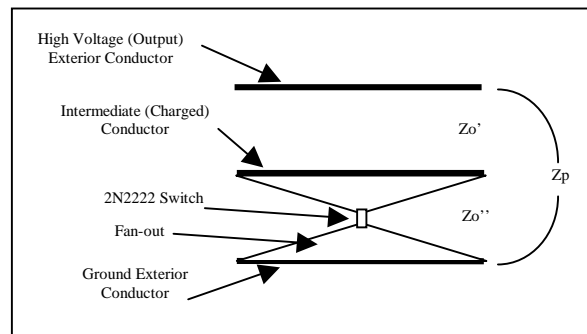


Figure 2: Experimental Blumlein cross section.

* Work supported by AFOSR under the DEPSCoR Program, Grant # F49620-02-1-0257 and in part by the Compact Portable Pulsed Power MURI.

B. Blumlein Design

The Blumlein is a type of vector inversion pulse generator that takes advantage of multiple transmission lines to generate a variety of waveforms based on the combination of impedances involved. Referring to Figure 2, it is composed of two exterior transmission line plates that ultimately form the output section of the Blumlein. An intermediate transmission line plate is placed between the two exterior plates and charged to V_c . A 2N2222 switch (ultimately a self-break Hydrogen switch) closes to electrically connect the intermediate plate to the bottom (in this case, ground) plate. The resulting transmission line signals generate a voltage pulse on the Blumlein output with pulse width equal to the two-way transit time of the intermediate conductor and an output voltage amplitude (V_o) approximately equal to V_c .

In this application, the Blumlein output impedance (the impedance between the exterior conductors with no intermediate conductor present) is selected to be approximately 100Ω . It has been shown that the output to charge voltage ratio (V_o/V_c) of a Blumlein is related to the ratio of the intermediate plate width to the exterior conductor plate widths [1]. Increasing the intermediate plate width with respect to the exterior plate widths increases the parasitic impedance (Z_p) and increases the output to charge voltage ratio (V_o/V_c) asymptotically toward unity. Experimental investigations have indicated that although increasing the intermediate conductor plate width does in fact increase the ratio V_o/V_c , the increased plate width may increase the rise time to maximum output voltage as compared to an intermediate plate equal in width to the two exterior conductors. For this application, an intermediate plate width equal to the exterior conductors was selected and compared with the performance of a switch with a center conductor 2.5 times wider than the outer conductors.

The Blumlein impedances were evaluated using the Electro software package [2]. Electro is a 2D electrostatics code that computes solutions to the Poisson equation, allowing the capacitance and inductance per unit length for the structure to be determined. A schematic of an Electro Blumlein model is shown in Figure 3. The dimensions of the Blumlein were selected to maintain the desired impedance as well as to accommodate the 1.5 cm tall gas switch which will ultimately be incorporated into the Blumlein. This will be referred to as the prototype arrangement. For the Electro analysis, the top and intermediate conductors were assigned as conductors 1 and 2 respectively and the bottom conductor is assigned as ground. The result of the Electro analysis is a capacitance matrix as shown in Table 1 below.

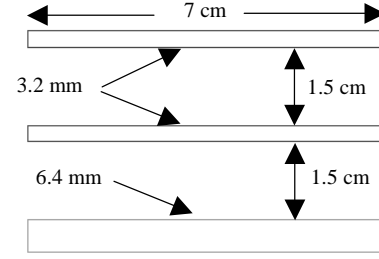


Figure 3: Blumlein Electro model cross section.

C	1	2
1	1.73E-11	1.47E-11
2	1.47E-11	2.96E-11

Table 1: The capacitance matrix for the multi-conductor transmission line in Figure 3.

Capacitance C_{11} is the total capacitance from conductor 1 to both conductor 2 and to ground. Capacitance C_{21} is the capacitance from conductor 1 to conductor 2 and, as should be the case in this configuration, C_{21} equals C_{12} . C_{22} is the capacitance from conductor 2 to both conductor 1 and to ground. The intermediate conductor is selected to be 30 cm long to generate a 2 ns output pulse. Therefore, the one-way transit time, τ , is 1.0 ns. From the capacitance matrix above, and referring to Figure 2, the relevant impedances are calculated as:

$$Z_{o'} = \frac{\tau}{C_{21}} = \frac{1e^{-9}}{1.47e^{-11}} = 68\Omega \quad (1)$$

$$Z_{o''} = \frac{\tau}{C_{22} - C_{21}} = \frac{1e^{-9}}{2.96e^{-11} - 1.47e^{-11}} = 67\Omega \quad (2)$$

$$Z_p = \frac{\tau}{C_{11} - C_{12}} = \frac{1e^{-9}}{1.73e^{-11} - 1.47e^{-11}} = 384\Omega \quad (3)$$

The total impedance from the top plate to the bottom plate within the Blumlein section can be calculated as:

$$Z_o = \frac{(Z_{o'} + Z_{o''}) * Z_p}{Z_{o'} + Z_{o''} + Z_p} = 100\Omega \quad (4)$$

Once the relevant impedances are known ($Z_{o'}$, $Z_{o''}$, Z_p), the performance of various Blumlein conductor configurations can be accurately predicted using Pspice [3]. A PSpice screen shot is shown in Figure 4 below. In Figure 4, T1 represents impedance $Z_{o'}$, T2 represents $Z_{o''}$ and T4 represents Z_p . T3 represents the Blumlein output impedance; the impedance of the exterior conductors without the intermediate conductor. According to Electro, the prototype arrangement output impedance is 107Ω .

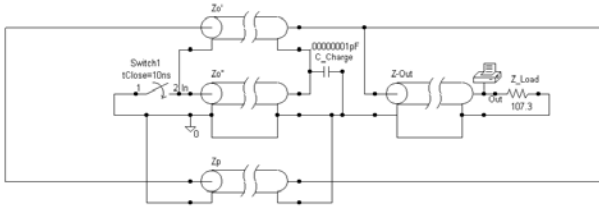


Figure 4: PSpice screen shot of Blumlein circuit.

III. SIMULATION AND EXPERIMENT

Table 2 presents the configurations that we tested in this paper. The various configurations had either a narrow or wide center conductor, and had the center conductor offset towards the top (positive offsets) or bottom (negative offsets) electrode.

Table 2: Configurations tested in this study.

Configuration #	Center Electrode Width	Center Electrode Offset
0	21 cm	0 cm
1	7 cm	0 cm
2	7 cm	-3.8 mm
3	7 cm	-7.6 mm
4	7 cm	-12.4 mm
5	7 cm	+12.4 mm

Figure 5 shows the cross section and the Electro predicted equipotential lines for configuration 5. The cross sections for the other tested configurations are similar, with the center conductor offset towards one of the outer electrodes. Note that there is field enhancement in the upper region, as expected, causing a decrease in the impedance of the upper transmission line and an increase in the impedance of the lower line. This unbalanced impedance causes the Blumlein to ring.

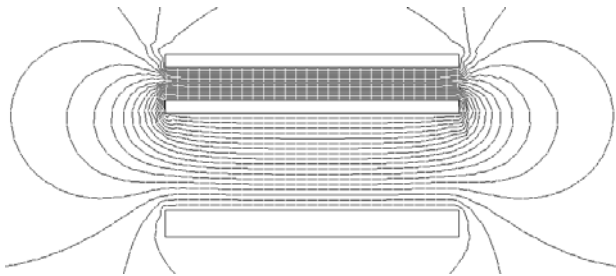


Figure 5: Cross section and equipotential line calculations for configuration 5 in table

Figure 1 shows the measured output voltage for configurations 0 and 1. This demonstrates the benefit of using a wider center conductor. Note from the figure that the Blumlein with the wide center conductor has an output voltage which is almost 100% of the charge voltage. In contrast, the Blumlein with the narrow center conductor has an output voltage of approximately 83% of the charge voltage. This is in agreement with earlier simulations [1].

However, there appears to be no rise-time penalty, at least at these rise time scales. This determination was made by normalizing the voltage waveforms in figure 6 (data not shown).

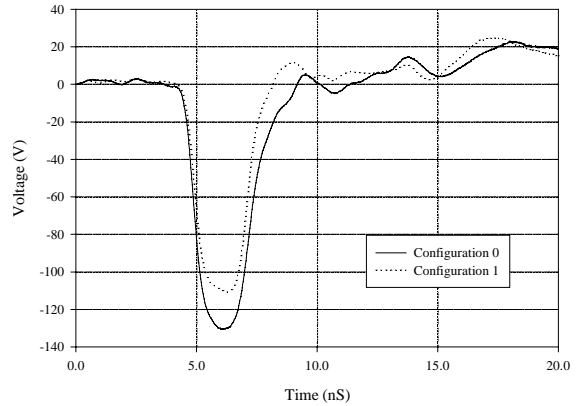


Figure 6: Measured output voltage waveforms in configurations 0 and 1.

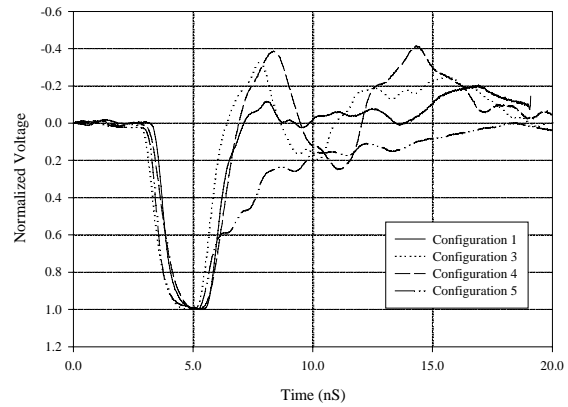


Figure 7: Measured voltage waveforms for some of the configurations shown in

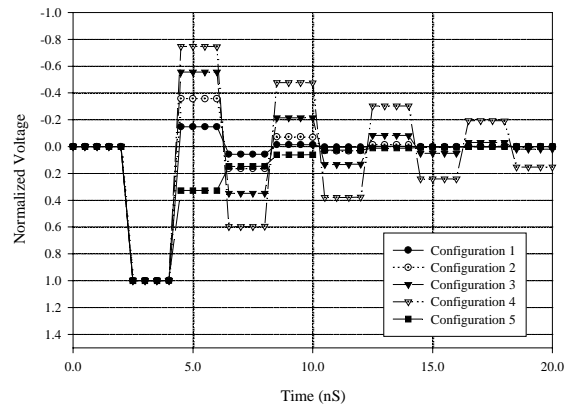


Figure 8: Pspice Simulated waveforms for configurations 1 through 5.

Figure 7 presents the measured, normalized output voltage waveforms for configurations 1, 3, 4, and 5. Note that the

output waveform varies between an exponential decay and an under-damped ringing waveform based only on the vertical location of the Blumlein center conductor. Figure 8 presents the corresponding Pspice simulations as well as a simulation for configuration 2. The trends predicted by the Pspice simulations are realized in the measured data, and the agreement is best for configuration 5. Both the polarity of the ringing and the approximate Q of the circuit is predicted by the model. Further experiments were undertaken to determine how well the center frequency of the output pulse can be adjusted by simply retracting the center plate axially from within the exterior plates as illustrated in Figure 9 below. In Figure 9, l_i refers to the length of center conductor still between the exterior conductors and l_o refers to the length of center conductor that has been retracted.

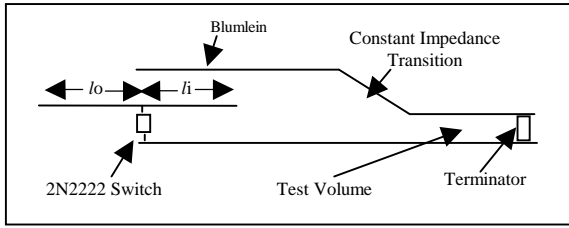


Figure 9: Adjusting Blumlein center frequency.

The experiment began with configuration 1 from above and the center conductor was retracted in 7.5 cm steps as listed in Table 3 below.

Table 3: Retracted center plate configurations.

Configuration #	l_i (cm)	l_o (cm)
1	30.0	0.0
6	22.5	7.5
7	15.0	15.0
8	7.5	22.5

The results of the experiment are given as Figure 10 below. As can be seen in the experimental results, re retracting the center conductor reduces the temporal width of the output pulse while the increased parasitic capacitance due to the center conductor extending outside the Blumlein section does not seem to have affected the overall performance of the Blumlein for these rise times.

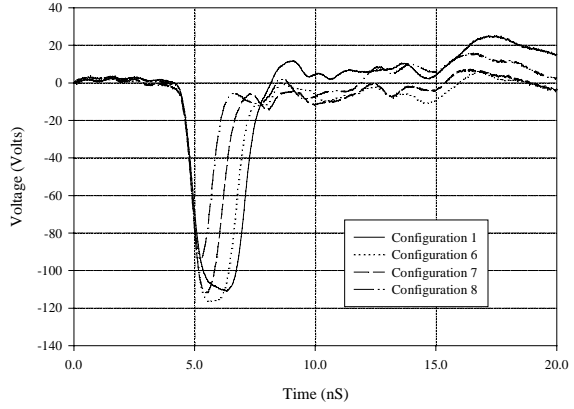


Figure 10: Retracted center plate measurements.

IV. CONCLUSIONS

It has been demonstrated through simulations and experiments that the damping factor, Q, and the center frequency of a Blumlein can be adjusted by changing only the vertical and axial location of the center plate. Therefore a very agile pulsed voltage source can be built around a Blumlein in which only one conductor is required to move. In future work, we will incorporate a hydrogen-based gas switch that will allow the device to be operated at higher voltages. The switch will be built in such a manner as to allow a sliding contact with the center conductor, enabling the tunability benefits discussed in this paper.

V. REFERENCES

[1] J. S. H Schoenberg, J. W. Burger, J. S. Tyo, M. D. Abdalla, M. C. Skipper, and W. R. Buchwald, "Ultra-Wideband Source Using Gallium Arsenide Photoconductive Semiconductor Switches," *IEEE Transactions on Plasma Science* **25**:327 – 334 (1997)

[2] Electro 6.1, Integrated Engineering Software Sales Inc., 220-1821 Wellington Avenue, Winnipeg, Manitoba, Canada R3H 0G4

[3] PSpice 9.1, Cadence Design Systems, Inc., 555 River Oaks Parkway, San Jose, CA 95134